Formation of Duct and Self-Focusing in Plasma by High Power Microwave

H. Ito,* Y. Nishida,[†] and N. Yugami[‡]

Department of Electrical and Electronic Engineering, Utsunomiya University,
2753 Ishii-machi, Utsunomiya, Tochigi 321, Japan
(Received 24 October 1995)

The optical guiding of an intense electromagnetic wave is demonstrated with the use of high power microwaves in a preformed plasma density channel. The high power microwaves make a duct into the overdense area by the ponderomotive force in a preformed density channel and are guided along the duct to remain within it. The parametric dependencies are investigated to be compared with the results obtained from numerical calculation, showing fairly good coincidence. [S0031-9007(96)00433-4]

One of the most interesting current topics is to develop high energy particle accelerators based on plasmas with short pulse lasers. A number of ways to excite plasma waves having gradients as high as several tens of GeV/m have been proposed so far for plasma based laser driven accelerators. The laser wakefield accelerator (LWFA) [1,2] is one of the most sophisticated ones, and the maximum acceleration gradients of 30 GeV/m have recently been observed [3]. The LWFA, however, has the fault that the acceleration distance is severely limited to the diffraction length, or Rayleigh length. The self-focusing [4] and the self-guiding (optical guiding) [2] of an intense electromagnetic wave (EMW) in a plasma have been proposed to overcome this limitation. The phenomena are particularly interesting for processes requiring long interaction lengths such as x-ray lasers [5], high harmonic generation [6], and laser-driven accelerators. More recently theoretical works and experimental results on optical guiding [7–10] have been presented.

One approach to the guiding of an intense EMW in a plasma depends on self-induced modulations of the plasma refractive index. There are two types of optical guiding mechanisms. One is self-optical guiding due to the ponderomotive force of an intense EMW and the other is optical guiding due to the relativistic effect. The former utilizes the dependence of the refractive index, N, on the plasma density, $N = \sqrt{1 - (\omega_p/\omega_0)^2}$, where ω_0 is the incident-wave frequency, $\omega_p = (4\pi n_e |e|^2/m_e)^{1/2}$ is the plasma frequency with popular notations. With the preformed density channel along the passage of EMW, it propagates in this channel over distances exceeding the Rayleigh length. The experimental demonstration of this phenomenon has been reported recently [9]. The second phenomenon results from the increase of the refractive index due to the relativistic quiver motion of electrons. Because the refractive index has the largest peak on the axis where the intensity of EMW is maximum, the refractive index distribution is the same as that of an optical fiber. Such relativistic self-focusing and self-guiding occur when the incident-wave power P exceeds the critical power $P_c = 16.2(\omega/\omega_p)^2$ GW [11,12].

In this Letter, we present the first experimental results of ducting of EMW using high power microwaves instead of an intense laser. We demonstrate that the microwave expands the preformed density channel with the ponderomotive force so that the EMW remains trapped in the channel and propagates along it in an overdense area. These results show the formation of ducting of the microwave in a plasma. We use a simple propagation model with the refractive index distribution similar to that of the optical fiber and compare with experimental results, showing fairly good agreement.

The experimental arrangement used in the present studies is shown in Fig. 1 [13]. The typical plasma parameters, measured by both a cylindrical probe with a tip of 1 mm length by 0.25 mm diameter and a plane probe with an area of 1×1 mm^2, are the electron density $n \leq 2.0 \times 10^{12}$ cm^{-3}, electron temperature $T_e \approx 3-5$ eV in an argon gas pressure $P = (3-4) \times 10^{-3}$ Torr. The typical density gradient scale length in the axial direction has $L_z = (\partial \ln n/\partial z)^{-1} \approx 100-120$ cm and in the radial direction, $L_r \approx 50-100$ cm near the axis.
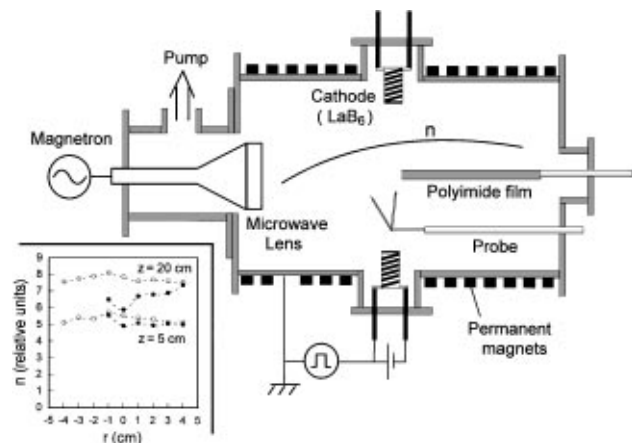

FIG. 1. Experimental apparatus used in the present studies. The inset shows the radial plasma density profile observed in an ion saturation current. Open circles and solid circles are without polyimide sheet and with the sheet, respectively.

The pulsed microwave, a frequency of $f_0 = 9$ GHz, maximum power of 250 kW, and pulse duration of 1 μsec, in full width at half maximum is irradiated from the rectangular horn antenna with a metal lens. The antenna is located at the lower end of the plasma density. The metal lens makes the ray trace of the incident microwave parallel along the propagation direction. Thus, the microwave is considered to be a plane wave, which has been confirmed in air without plasma. The ratio of the electric field energy to the plasma energy is estimated to be $\eta \equiv \varepsilon_0 E_0^2 / 4 n_0 k_B T_e \approx 0.5$, where E_0 is the maximum electric field intensity of the incident microwave measured at the outlet of the horn antenna, n_0 is the electron density there, and k_B is Boltzmann's constant.

The density channel is formed by inserting a polyimide film sheet with 240 mm length by 15 mm width and 125 μm thickness at the center of the chamber along the plasma axis. In the present experiments, the sheet is inserted from the higher density side up to 15 cm from the edge of the metal lens. An example of the spatial distribution of the density channel is shown in the inset of Fig. 1, which shows that the plasma density is uniform in a radial direction without the sheet, while the density channel is formed with the sheet. We estimate that the width of the density channel perpendicular to the electric field, E_y, is less than about 1 cm, which is small enough compared with the cutoff wavelength of the fundamental TE mode of the standard waveguide.

When the microwave pulse is injected into this density channel, it makes a hole by expanding the plasma via the ponderomotive force and propagates into the higher density side. A typical example is shown in Fig. 2, which represents an axial profile of the electric field pattern taken along the direction of the propagation (z direction) as a parameter of an incident power with the density profile. In Fig. 2(a) observed on the axis, you may recognize three peaks (α, β, γ) with the spatial separation of about 2.2 cm. These peaks disappear in the lower incident power, though we do not show the results in Fig. 2. Note that without plasma in the present chamber the strong standing wave

structure has been formed with peak separation typically 1.6 cm, and the phenomena are clearly different from those of $\alpha \sim \gamma$ peaks. On the other hand, these peaks disappear outside of the channel. In the low enough power case without the sheet, there is a cutoff layer on the axis at $z = 16$ cm, while with the sheet the cutoff layer exists around $z = 17$ cm outside of the channel [see Fig. 2(b)]. Thus, we can say that the electric field is confined around the axis as the microwave pulse penetrates along the channel up to a certain area where η becomes so small that the wave is cut off, because the pump wave is depleted and the ponderomotive force becomes weaker not to expand the plasma any more, resulting in the wave reflection at $z \simeq 20$ cm, not to go through into the overdense area. It is well known that the wavelength (λ_g) of the fundamental TE mode in the standard waveguide is $\lambda_g \simeq 4.8$ cm. If we assume that the microwave pulse in the density channel is the fundamental TE mode, the standing wave structure with spatial separation of about 2.2 cm is formed in the density channel.

Figure 3 shows typical examples of the density depletion during the microwave pulse irradiation. As seen in Fig. 3(a), the density decreases to about 0.57 from 0.72; the initial value, when the microwave power is small, while in Fig. 3(b), decreases to about 0.3; 40% of the initial value, and the phase relation between density n and the electric field $|E|^2$, becomes almost out of phase. After shutting off the microwave pulse, density increases slightly in the longer pulse operation, but not all the time. This may come from a small amount of ionization of the background neutral gases. The effect from the ionization is not serious at all for the present channeling effect, although additional power depletion by the ionization may result.

Figure 4 shows the transverse profile of the microwave field strength observed at $z = 17$ and 19 cm, respectively. As the microwave power increases, the propagation area shrinks to the axis, and the wave propagates farther into the overdense area. Here, the experimental values are normalized at $r = 0$ cm.
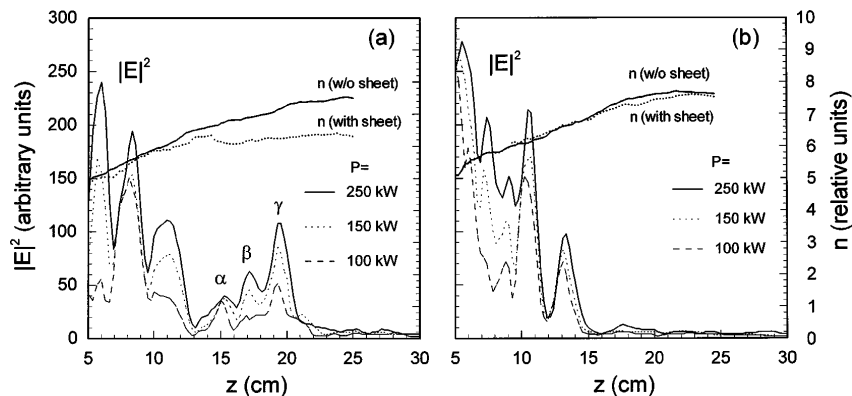

FIG. 2. Profiles of the time averaged $|E|^2$ and density profile without microwave as a function of the axial distance measured at radial positions (a) $r = 0$ cm and (b) $r = 4$ cm.
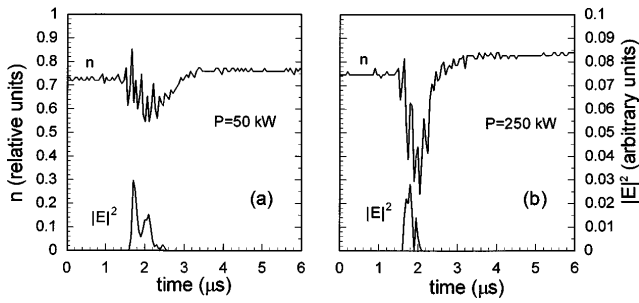
FIG. 3. Examples of electron density perturbation and electric field at $z = 20$ cm. Incident powers are (a) $P = 50$ kW and (b) $P = 250$ kW, respectively.
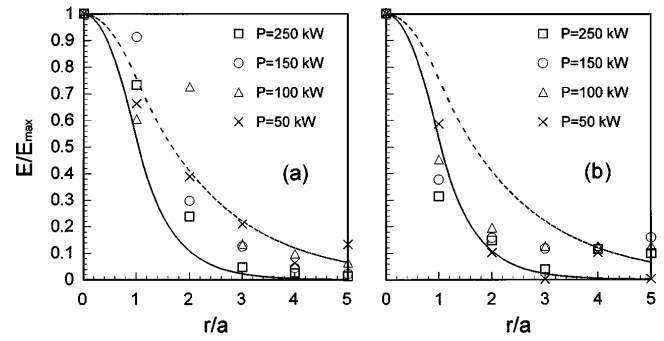

FIG. 4. Normalized radial field profiles as a parameter of the incident microwave power. Solid and dashed curves represent numerical results. The parameters are channel radius $a = 1$ cm, refractive index $N_2 = 0$, and $N_1 = 0.5$ for dashed line and $N_1 = 1$ for solid line. Axial positions are (a) $z = 17$ cm (lower density) and (b) $z = 19$ cm (higher density).

Figure 5(a) shows the experimental results of the half width at half maximum (HWHM) of the radial field intensity profile Δr as a function of the axial distance and the incident microwave power. The half-width Δr changes along the channel to be minimum around $z \simeq 20$ cm as seen in Fig. 5(a), while the field amplitude becomes maximum on the axis [see Fig. 2(a)]. The increase of the microwave power makes Δr smaller. From these results, we can say that the microwave pulse is focused at $z \simeq 20$ cm, even though the incident microwave has almost parallel ray trace. Figure 5(b) shows HWHM measured at each axial position as a function of the incident power. If the refractive index did not vary along the channel even if the incident power changed, the half-width should remain constant. However, it is evident from Fig. 5(b) that the half-width tends to decrease with the increase of the incident power. Thus, the effects from the variation of refractive index are very important to take into account in the theoretical analysis.

In order to interpret the observed behavior, a transverse profile of the microwave field strength is calculated in the density channel, after assuming that the microwave pulse is so weak that the relativistic effect can be neglected, and the plasma is modeled using nonrelativistic cold fluid equations. Here, one can employ a propagation model approximated in an optical fiber with refractive indexes N_1 inside and N_2 outside. Because the microwave field can be assumed to be axially symmetric, the fundamental TE mode solution of Maxwell's equations is looked for. In slab geometry, this solution [14] is given by

$$E_y = \begin{cases} E_0 \cos(k_x x) \exp(-jkz) & (|x| \leq a), \\ E_0 \cos(k_x a) \exp[-p(|x| - a)] \exp(-jkz) & (|x| > a), \end{cases} \quad (1)$$

where $k_x^2 = N_1^2 k_0^2 - k^2$, $p^2 = k^2 - N_2^2 k_0^2$, and $k_0 = \omega_0/c$, c is the speed of light, and a is the channel radius, which is a function of z. Applying the continuity condition of magnetic field H_x in two regimes (N_1 and N_2), one obtains the characteristic equations

$$p = k_x \tan(k_x a), \qquad p^2 + k_x^2 = k_0^2(N_1^2 - N_2^2). \quad (2)$$

Equation (2) can be solved numerically for k_x at a certain constant position of z as a function of the refractive index N_1, N_2, and the channel radius a. The channel radius is assumed to be $a = 1$ cm at $z = 20$ cm from the experimental result. Because the plasma density outside of the channel is overdense, we may put $N_2 = 0$. The calculated results for the above-mentioned conditions are plotted in Fig. 4. Here, the solid line and the dashed line are obtained for the case of $N_1 = 1$ (in vacuum) and $N_1 = 0.5$, respectively. Here, $N_1 = 0.5$ is estimated from a density decrease due to the insertion of the sheet. You may see that the experimental results at the lower density [Fig. 4(a)] show better agreement with the numerical result of $N_1 = 0.5$ than that of $N_1 = 1$, while at the higher density [Fig. 4(b)] the experiments are closer to the $N_1 = 1$ case. These results can be understood as follows.
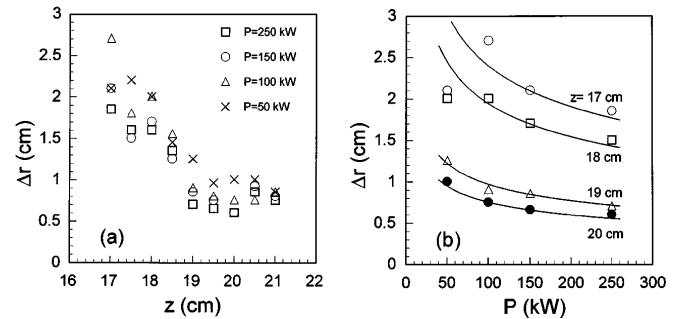

FIG. 5. Half width at half maximum of radial field profile Δr, as a function of the axial distance in (a) and as a function of the incident power in (b). Solid lines in (b) represent theoretical results fitted to the experiments at $P = 150$ kW for $k = 26$ at $z = 17$ cm, 21 at $z = 18$ cm, 10 at $z = 19$ cm, and 8 at $z = 20$ cm, respectively.

As the microwave propagates along the plasma channel, the electric field in the channel is maximum around $z = 20$ cm. The refractive index of the channel changes gradually to $N_1 \rightarrow 1$ along the plasma channel; i.e., the channeling rate varies along the pulse propagation, since electrons in the channel are pushed out of the channel by the enhanced ponderomotive force. This consideration has been confirmed by experiments in which density dips due to the ponderomotive force appear just when the microwave pulse is irradiated. Considering that the density decreases to about 75% at $z = 20$ cm due to the insertion of the sheet and then that the microwave pulse with the incident power $P = 250$ kW makes a further decrease to (30–40)% of the original density with digging a hole on the axis by the additional ponderomotive force (see Fig. 3), we can estimate that the refractive index of the channel is $N_1 = (1 - \omega_p^2/\omega^2)^{1/2} \simeq 0.8$. This estimation demonstrates that the experimental results are interpreted by the theoretical calculation of the case of $N_1 = 1$ as the microwave propagates farther into the channel. Thus, the results indicate the existence of ducting of the microwave along the preformed density channel.

The half-width of the radial field profile is estimated to be $\Delta r \simeq 1/k_x$. Equation (2) leads to $k_x/\cos[k_x a(z)] = N_1 k_0$. It can be approximated that the transverse wave number k_x is directly proportional to the refractive index N_1, since $\cos(k_x a)$ varies little during the microwave propagation into the channel. Therefore, the half-width is approximated by $\Delta r \simeq 1/k_x \sim 1/N_1$. The channel refractive index is given by $N_1 = (1 - n/n_c)^{1/2} = (\delta n/n_c)^{1/2}$, where $n = n_c - \delta n$. Using the momentum and continuity equations and taking $P = S|E|^2/Z_p$ at a certain location into account, one can show that the refractive index N_1 is directly proportional to $P^{1/3}$, where S is a cross section of the channel, $Z_p = Z_0/N_1$ is a characteristic impedance of the microwave inside the channel, and Z_0 is the characteristic impedance in vacuum. Thus, the half-width is given by

$$\Delta r = K/P^{1/3}, \tag{3}$$

with some constant K that depends mainly on the interaction duration and the wavelength of the electromagnetic wave. This result is plotted in Fig. 5(b) by solid lines after fitting the numerical results to the experiments at $P = 150$ kW with a different K value for each location. The results show fairly good agreement.

In conclusion, we have demonstrated that the ducting of the microwave is formed and the microwave pulse remains trapped and guided in the plasma channel at the fundamental TE mode. However, as the ponderomotive force is not strong enough, the wave is reflected back at a certain location and the standing wave structure is formed within the channel. The comparisons of the half-width Δr of the experimental observations with the theoretical calculations show fairly good agreement for both the transverse profile of the electric field and its dependence on the incident power. The experimental results can be explained by the concept of "optical guiding."

*Electronic address: t3952051@cc.utsunomiya-u.ac.jp
†Electronic address: nishiday@cc.utsunomiya-u.ac.jp
‡Electronic address: yugami@cc.utsunomiya-u.ac.jp

[1] T. Tajima and J. M. Dawson, Phys. Rev. Lett. **43**, 267 (1979).
[2] P. Sprangle, E. Esarey, A. Ting, and G. Joyce, Appl. Phys. Lett. **53**, 2146 (1988).
[3] K. Nakajima, D. Fisher, T. Kawakubo, H. Nakanishi, A. Ogata, Y. Kato, Y. Kitagawa, R. Kodama, K. Mima, H. Shiraga, K. Suzuki, K. Yamakawa, T. Zhang, Y. Sakawa, T. Shoji, Y. Nishida, N. Yugami, M. Downer, and T. Tajima, Phys. Rev. Lett. **74**, 4428 (1995).
[4] C. E. Max, J. Arons, and A. B. Langdon, Phys. Rev. Lett. **33**, 209 (1974); W. Mori, C. Joshi, J. M. Dawson, and J. M. Kindel, Phys. Rev. Lett. **60**, 1298 (1988).
[5] N. H. Burnett and P. B. Corkum, J. Opt. Soc. Am. B **6**, 1195 (1989); P. Amendt, D. C. Eder, and S. C. Wilks, Phys. Rev. Lett. **66**, 2589 (1991).
[6] X. F. Li, A. L'Huillier, M. Feray, L. A. Lompré, and G. Mainfray, Phys. Rev. A **39**, 5751 (1989).
[7] P. Sprangle, E. Esarey, J. Krall, and G. Joyce, Phys. Rev. Lett. **69**, 2200 (1992); E. Esarey, P. Sprangle, J. Krall, A. Ting, and G. Joyce, Phys. Fluids B **5**, 2690 (1993).
[8] T. M. Antonsen, Jr. and P. Mora, Phys. Fluids B **5**, 1440 (1993); Phys. Rev. Lett. **74**, 4440 (1995).
[9] C. G. Durfee III and H. M. Milchberg, Phys. Rev. Lett. **71**, 2409 (1993).
[10] P. Monot *et al.,* Phys. Rev. Lett. **74**, 2953 (1995); P. E. Young *et al.,* Phys. Rev. Lett. **75**, 1082 (1995).
[11] G. Schmidt and W. Horton, Comments Plasma Phys. Controlled Fusion **9**, 85 (1985).
[12] G. Z. Sun, E. Ott, Y. C. Lee, and P. Guzdar, Phys. Fluids **20**, 526 (1987); P. Sprangle, C. M. Tang, and E. Esarey, IEEE Trans. Plasma Sci. **15**, 145 (1987).
[13] X. Xu, Y. Nishida, and N. Yugami, J. Plasma Fusion Res. **72**, 91 (1996).
[14] Donald L. Lee, *Electromagnetic Principles of Integrated Optics* (Wiley, New York, 1986), Chap. 4; T. C. Chiou, T. Katsouleas, C. Decker, W. B. Mori, J. S. Wurtele, G. Shvets, and J. J. Su, Phys. Plasmas **2**, 310 (1995).